

EVALUATION OF INTRACEREBRAL HAEMORRHAGE'S SURFACE AREA USING ARTIFICIAL INTELLIGENCE IN COMPUTED TOMOGRAPHY

Azzam Basseri Huddin¹, Aqilah Baseri Huddin², Anas Tharek^{*1}, Wan Mimi Diyana Wan Zaki², Ahmad Sobri Muda¹

¹Department of Radiology, Hospital Pengajar Universiti Putra Malaysia, Universiti Putra Malaysia, Faculty of Medicine and Health Sciences, Universiti Putra Malaysia, Serdang, Malaysia

²Department of Electrical, Electronic and Systems Engineering, Faculty of Engineering and Built Environment, Universiti Kebangsaan Malaysia, Bangi, Malaysia

*Corresponding author:

Anas Tharek, Department of Radiology, Hospital Pengajar Universiti Putra Malaysia, Universiti Putra Malaysia, Faculty of Medicine and Health Sciences, Universiti Putra Malaysia, Serdang, Malaysia. Email: anastharek@gmail.com

DOI: <https://doi.org/10.32896/cvns.v4n3.1-13>

Submitted: 15.06.2022

Revised: 14.08.2022

Accepted: 29.09.2022

Published: 30.09.2022

ABSTRACT

Introduction: AI-based techniques can be used to localize and measure the intracerebral haemorrhage (ICH) in computed tomography (CT). This study aims to develop an automated detection algorithm with higher sensitivity in ICH evaluation in comparison to the conventional method. This indirectly influences the patient's prognosis by reducing the risk of delay or misdiagnosis.

Methods: Selected 50 CT brain images with primary ICH were used for three different measurement approaches including the conventional Kothari method (Conventional), AI-based method (A.I.), and manually marking by the radiologist, which is the ground truth (G.T.). In the automated system, a convolutional neural network (CNN) is used to localize the ICH, followed by a thresholding technique to segment the ICH, and finally, the measurements are computed. The segmentation performance is measured using Dice similarity coefficient. The automated ICH measurements are compared against the ground truth (A.I. vs G.T.). Concurrently, the ICH measurements calculated using the conventional method are also compared against the ground truth (Conventional vs G.T.). The t-test analysis is performed between the sum squared error (SSE) of ICH measurements from the automated-ground truth and the conventional-ground truth.

Results: The mean volumetric Dice similarity coefficient for the automated segmentation algorithm when tested against the ground truth, is 0.859 ± 0.135 . The t-test analysis of the SSE between conventional-ground truth (median=5.45, SD=3.96) and automated-ground truth (median=0.73, SD=0.78) achieved p-value < 0.001 ($p=5.10E-9$).

Conclusion: The automated AI-based algorithm significantly improved the ICH surface area measurement from the CT brain with higher accuracy and efficiency in comparison to the conventional method.

Keywords: Artificial Intelligence; Machine learning; Radiology; Neurology; CT Brain

INTRODUCTION

One of the most common brain pathologies is intracranial haemorrhage. It is defined as any bleeding episode within the brain or cranial vault. It can be divided into a few categories, which are based on the acuteness of the blood formation and the spaces involved. This categorization is important, as it plays a crucial role in determining the severity of the bleeding and treatment options, as well as predicting the outcomes [1].

Based on brain locations or spaces the bleeding occurs, it can be divided into intra-axial and extra-axial haemorrhage. Intraaxial haemorrhage is defined as bleeding which occurs in the brain, which is intracerebral haemorrhage, while extra-axial haemorrhage is bleeding which occurs outside of the brain parenchyma, which is subdural, subarachnoid, and epidural haemorrhage. Worsening of the patient's condition is usually due to secondary complications from intracranial bleeding, such as increases in the intracranial pressure, hydrocephalus, and significant midline shift.

Thus, the initial treatment option is crucial in improving patient prognosis and outcomes. Hence, a supportive measure such as prompt brain screening using computed tomography (CT) or magnetic resonance imaging (MRI) scan is helpful, to prevent any delay management.

Meanwhile, implementing artificial intelligence, aiming to aid the radiologist or physician in the detection of intracranial haemorrhage [2], may further reduce the risk of delay or misdiagnosis.

METHODS

Study Design

This was a cross-sectional Computed Tomography (CT) head study using primary raw data, in which the data was obtained from patient who was admitted to Hospital Serdang and underwent a non-enhanced CT brain examination in Radiology Department for further investigation. The data was checked to comply with the inclusion and exclusion criteria before taken as samples for this study. No consent was taken as this is a retrospective study and all the data are anonymized to secondary data.

Sampling Method

The population of this study consists of patients who

were admitted and underwent non-enhanced CT brain for intracerebral haemorrhage, and within the inclusion criteria. The patient would present with common symptoms, including headache, hypertension, loss of consciousness, vomiting, or neurological deficit. The sample includes CT brain with intracerebral haemorrhage (ICH). The sample of CT Brain also needs to have formal radiologist report, to prevent from using uncertain brain pathology as the subject. Other types of intracranial haemorrhage, such as epidural or subdural haemorrhage (EDH & SDH).

Sampling Size

This study aims to determine a high level of agreement between readings obtained from A.I. and conventional methods. It is recommended to pre-specify a high value (for intraclass correlation coefficient (ICC) at 0.90 in the null hypothesis and a higher value (for ICC) at 0.95 in the alternative hypothesis). This is to ensure that the study has indicated that a minimum level of agreement as shown by ICC = 0.90 is expected in the first place, but the aim is to establish that the targeted level of agreement should be much higher, as shown by the value of ICC which exceeds 0.95. Therefore, based on only two observations made on each subject, a sample size of at least 50 is required to achieve statistical significance for an alpha-value set to be 0.05 and with a power of more than 80.0% [3].

Data Collection, Instruments and Quality Control

The CT head was scanned using a CT machine (Siemens Somatom 128 Slices) located in the Radiology Department Hospital Serdang of patients who are having ICH and complying with inclusion criteria. Data or images were then transferred to GE Centricity PACS UV software (version 6.0). for viewing. This data is downloaded from the PACS system in DICOM format and kept on a workstation computer. Personal information was filtered out or deleted during the process to anonymize the subject. These data were duplicated and placed into three separate folders, which are for A.I.-based automated evaluation, manual demarcation (Ground Truth), and conventional measurement, derived from Kothari's ABC/2 method.

In this project, MATLAB (version R2020a Update 3) is used as the software for developing the algorithm with the license number 40925593.

MATLAB is a numeric programming platform widely used to program a complex computing model.

Intracranial Hemorrhage Measurement Method

Three types of ICH measurement techniques were conducted, which are conventional measurement derived from Kothari's method, a calculation from manual demarcation method, and fully automated measurement by A.I-based technique [4].

The calculation is derived from the ABC/2 method proposed by Kothari et al. in 1996. However, only the first step, which is the two dimensions were taken. They are the largest diameter (A) of hemorrhage on the axial slice, and the largest diameter (B) at 90 degrees to plane A as shown in **Figure 1**. The multiplication of these two dimensions is the estimated surface area of ICH. The reason for extracting only the first step of Kothari's method is because this study which only focuses on surface area measurement.

The manual measurement of ICH is made using RadiAnt (version 2020.1.1) or Osirix (version 11.0) viewer application. This software is compatible with Windows or Macintosh operating systems, respectively. In this viewer, the CT images are displayed, and the surface area was calculated manually by defining the length of A and B. However, this estimation is inaccurate since the formulation of A times B defines the area of a rectangle instead of the real area of ICH. The volume estimation using this method has been proven to demonstrate apparent inaccuracy, especially in significantly large hematoma, as it tends to underestimate its volume [5]. This has indirectly increased the odds of poor outcomes.

The second method for surface area measurement is performed in a hybrid way and hence the measurement is said to be 'semi-automatically' done. The ICH area is manually demarcated by the trained radiologists and the surface area is automatically calculated by the MATLAB software.

The demarcation process involved the conversion of CT images into compatible file types (JPEG), to be opened in photo editing software, which are Photos or Notability (version 10.4.2) applications on iPad Pro 10.1 (iPadOS 14). The margin is drawn by two different trained radiologists. **Figure 2** shows an example of two ICH markings from two different radiologists on the same CT

image in red color ink.

The next step is to calculate the area of the marked ICH. The measurement is made using the MATLAB software by calculating number of pixels included in the marked area. The automated ICH measurement algorithm is implemented based on AI techniques. The algorithm includes 4 important steps, 1) pre-processing, 2) segmentation, 3) ICH localization and detection 4) measurement.

In the pre-processing step, the images were pre-processed and normalized via the histogram normalization technique. This step is performed to achieve a standard range of pixels value in all images from 0 (black) to 1 (white). This is important to ensure the consistency of data distribution in the dataset.

After an image is pre-processed, the next step is to exclude the outer skull by a segmentation process. The algorithm used for the segmentation step is known as pixel thresholding. In the thresholding method, the algorithm will choose a set of threshold values to separate the pixel intensity into sets of desired regions. The threshold values are determined by defining the pixel values that separate the peaks of the histogram as shown in **Figure 3**. From the figure, since there are three peaks, the image pixels can be categorized into three main regions.

Figure 4(a) illustrates the original image that shows the 3 main regions (black, gray, and white) for thresholding. **Figure 4(b)** is the enhanced image and **Figure 4(c)** is the skull removed image. The purpose to remove the outer skull is to increase the sensitivity of the ICH detection algorithm by eliminating the pixels that have a similar range of density to the ICH.

Next step, the ICH in the segmented image is located using the state-of-the-art A.I-based technique, called deep neural network. Deep neural network is a type of machine learning, which consists of multiple levels of processing layers. These layers are to learn various extracting features through levels of abstraction. These enable machine learning of overly complex features from high-dimensional raw data [6]. There are several types of deep neural network, and in this project, a network called convolution neural network (CNN) is employed to detect and localize ICH on CT images [7].

CNN, or known as ConvNet, is a better option and is always considered above others. It has a deep feed-forward architecture, which contributes to its high learning efficiency in abstracting and identifying

features [8]. It is commonly used in image, voice, and text recognition and computer identification. It has a great feature of weight sharing and dimension reduction, which is the reason for its high effectiveness and efficiency, and low error rate [9].

Finally, after the ICH is located on the CT image, a rectangular shape containing the ICH is cropped. This step is important, to reduce the computational cost by performing further processing on the selected area only and avoiding any unnecessary processes. Using the same technique in skull removal, the thresholding method is applied to transform the cropped image into black and white, where the black area is the background, and the white area covered the ICH area. Thus, the ICH area can be markedly margined and identified, and hence the surface area is measured. **Figure 5** shows the result of a CT image after (a) ICH detection and localization in a coordinate, which is then marked in (b-c) yellow box containing (d) segmented ICH using ICH binary thresholding.

Data Analysis

The performance of the developed A.I. system to calculate the accuracy of the A.I.-based surface area measurement. The accuracy of the surface area was measured using the mean volumetric Dice similarity coefficients. The Dice similarity coefficients (DSC) measure the similarity between two datasets; hence the automatically segmented area was tested against the ground truth. DSC is shown in Equation (1).

$$DSC = (2 | X \cap Y |) / (| X | + | Y |) \quad (1)$$

where $|X|$ and $|Y|$ are the cardinalities of the two sets (i.e., the number of elements in each set). This index equals twice the number of elements common to both sets divided by the sum of the number of elements in each set. Equation (1) also can be:

$$DSC = 2TP / (2TP + FP + FN) \quad (2)$$

where TP is true positive, FP is false positive, and FN is false negative.

In the second stage, the statistical evaluation was performed by the sum of squared estimated of errors (SSE) between automated algorithm against ground truth, and SSE between conventional method against ground truth. The errors between these two

methods were analyzed using T-test to validate the significant improvement of the developed fully automated system. The SSE calculations follow the following equation:

$$SSE = \sum_{i=1}^n (x_i - x)^2 \quad (3)$$

where n is the number of observations, x_i is the value of the i -th observation, and x is the mean of all the observations.

RESULTS

Accuracy of Surface Area Measurement Using A.I.-Based Against Conventional Method

The system performance of the ICH surface area measurement is evaluated in two statistical analyses. The first analysis is performed to evaluate the similarity index of the detected ICH area against the manually marked area by the trained radiologists. **Figure 6** shows the ICH images (a) segmented based on marking by the radiologist and (b) automated detected and segmented by the A.I. system. Whilst in **Figure 6(c)**, the green line represents the non-overlapping pixels between the two segmented images. **Table 1** shows the result of dice similarity coefficients of the detected ICH, which achieved a mean sensitivity of 0.859 ± 0.135 .

The second statistical analysis is performed to measure the significance of the developed A.I.-based system as compared to the conventional method in terms of the accuracy of the measured surface area. The sum of squared estimated errors (SSE) between automated algorithm against ground truth (A.I. vs G.T.) and SSE between conventional method against ground truth (Conventional vs G.T.) was plotted as shown in **Figure 7**. The SSE for A.I. vs G.T. is median of 1.64 and standard deviation (SD) of 6.61. Meanwhile, the result for conventional vs G.T. was median of 49.62 and standard deviation (SD) of 60.09 (**Table 2**).

The t-test between both measurements is performed and has demonstrated good achievement of p-value of <0.001 (5.10×10^{-9}). This shows that the ICH surface area measurement using an automated AI-based system is significantly improved compared to the conventional Kothari's calculation method.

DISCUSSION

Medical error and misdiagnosis have been an inherent

part of medical practice. It can result in adverse impact on patient prognosis and recovery. It has been reported that the potential interpretation error rate in radiology is approximately 4% every year [10]. This may cause serious complications and delayed management of the patient.

There were many technologies and software developed previously to assist physicians and radiologists, in a way to reduce the margin of error. One of these is Computer Assisted Detection (CAD) in radiographic imaging and mammogram. A study has reported that CAD has an approximately 85% - 92% of accuracy in the detection of breast cancers on mammogram [11].

Artificial intelligence is another leap forward in better and developing medical technologies. Recently, many studies have undergone to create an artificial automated algorithm for detecting pathological findings in radiology and implemented it in a real hospital environment [12]. Some of these studies have also achieved approval from regulatory authorities such as the U.S. Food & Drug Administration (FDA), which considered it safe and beneficial to be used [13].

In this study, we report an A.I-based automated evaluation with accuracy comparable to that of a radiologist and conventional method of intracerebral hemorrhage on head CT. Head CT interpretation is regarded as a core skill in radiology training. The performance bar for this is accordingly high.

We demonstrate that this algorithm has achieved an adequate level of sensitivity in measuring the surface area of ICH. However, a higher rate of sensitivity may be achieved, if we used a larger number of samples to train the deep learning convolutional neural network. Future studies may be needed to further develop an enhanced version of this algorithm.

In comparison to the conventional method derived from Kothari ABC/2, this algorithm has proven to be better in accuracy with a lower error sum of squares. It shows that the measurement using this algorithm would be more precise and accurate, in comparison with the conventional and rudimentary way. This potentially gives a better insight into the patient's ICH severity, risk stratification, the cost-effectiveness of imaging tests, and better planning for optimal management.

Our future project on developing an algorithm with higher sensitivity of detection and improvement in a way of volume detection, rather than surface area, will be useful for deriving a more accurate measurement from head CT. This algorithm also can be implemented in future studies on other imaging modalities, and the detection of other types of lesions such as tumors or abscesses.

CONCLUSION

Unenhanced computed tomography of the brain is a reliable imaging technique to detect intracerebral hemorrhage. However, using the conventional and rudimentary way has a risk of delay or misdiagnosis. This A.I-based automated ICH measurement algorithm may contribute greatly to the patient's management. At the same time, it may aid and reduces the burden on the radiologist or physician.

STATEMENT OF ETHICS

A written ethical approval and permission have been obtained from Medical Research & Ethic Committee (MREC), Ministry of Health Malaysia on 4th February 2021 for a period of one year. The reference number is NMRR-20-2860-54647 (IIR).

ACKNOWLEDGEMENTS

The authors would like to acknowledge Halimaton Khadijah Mohamad, who also had kindly provided guidance when required.

CONFLICT OF INTEREST

The author(s) declare that they do not have any potential conflicts of interest concerning the research, authorship, and/or publication of this article with anyone

FUNDING

No funding received for this project.

DATA AVAILABILITY STATEMENT

The data used in this work can be requested from the corresponding author upon reasonable request.

REFERENCES

1. Caceres JA, Goldstein JN. Intracranial hemorrhage. Emergency medicine clinics of North America. 2012 Aug 1;30(3):771-94.
2. Tharek A, Muda AS, Hudi AB, Hudin AB.

- INTRACRANIAL HEMORRHAGE DETECTION IN CT SCAN USING DEEP LEARNING. *AJMedTech*. 2022 Jan 31;2(1):1-8.
3. Bujang MA, Baharum N. A simplified guide to determination of sample size requirements for estimating the value of intraclass correlation coefficient: a review. *Arch. Orofac. Sci*. 2017 Jan 1;12(1).
 4. Danovska MP, Alexandrova ML, Totsev NI, Gencheva II, Stoev PG. Clinical and neuroimaging studies in patients with acute spontaneous intracerebral hemorrhage. *J of IMAB—Annual Proceeding Scientific Papers*. 2014 Mar 28;20(2):489-94.
 5. Delcourt C, Carcel C, Zheng D, Sato S, Arima H, Bhaskar S, Janin P, Salman RA, Cao Y, Zhang S, Heeley E. Comparison of ABC methods with computerized estimates of intracerebral hemorrhage volume: The INTERACT2 study. *Cerebrovasc. Dis. Extra*. 2019;9(3):148-54.
 6. Zamani NS, Zaki WM, Huddin AB, Hussain A, Mutalib HA, Ali A. Automated pterygium detection using deep neural network. *IEEE Access*. 2020 Oct 13;8:191659-72.
 7. Indolia S, Goswami AK, Mishra SP, Asopa P. Conceptual understanding of convolutional neural network—a deep learning approach. *Procedia computer science*. 2018 Jan 1;132:679-88.
 8. Zhang Z. Derivation of backpropagation in convolutional neural network (cnn). University of Tennessee, Knoxville, TN. 2016 Oct 18;22:23.
 9. Zhou X. Understanding the convolutional neural networks with gradient descent and backpropagation. *JPCS*. 2018 Apr 1;1004(1):012028)
 10. Waite S, Scott J, Gale B, Fuchs T, Kolla S, Reede D. Interpretive error in radiology. *AJR*. 2017 Apr;208(4):739-49.
 11. Brem RF, Hoffmeister JW, Zisman G, DeSimio MP, Rogers SK. A computer-aided detection system for the evaluation of breast cancer by mammographic appearance and lesion size. *AJR*. 2005 Mar;184(3):893-6.
 12. Tharek A, Muda AS, Huddin AB, Rahim EA, Git KA, Sabri MI, Abdullah R. Padimedical: Medical Image Sharing Portal with DICOM Viewer—User Experience. *International Journal of Human and Technology Interaction (IJHaTI)*. 2020 Oct 31;4(2):1-4.
 13. Benjamins S, Dhunoo P, Meskó B. The state of artificial intelligence-based FDA-approved medical devices and algorithms: an online database. *NPJ Digit*. 2020 Sep 11;3(1):1-8.

FIGURE LEGENDS

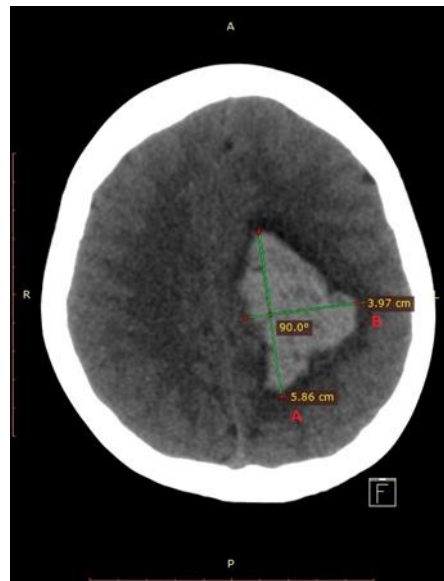


Figure 1: Conventional measurement of surface area, derived from the Kothari method. The largest diameter (A) multiplies with the largest diameter (B) 90 degrees to plane A.

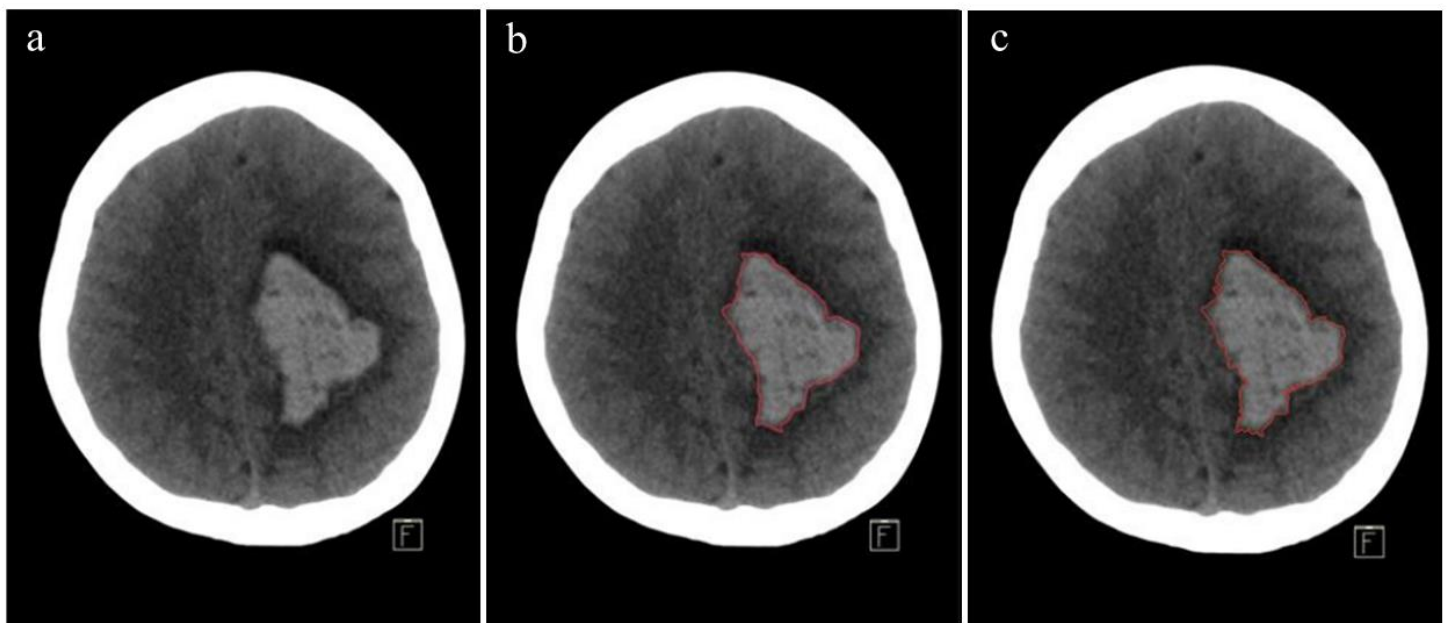


Figure 2: Manual demarcation by trained radiologists: (a) Pre-marking JPEG, (b) marking at #1 JPEG and (c) marking at #2 JPEG.

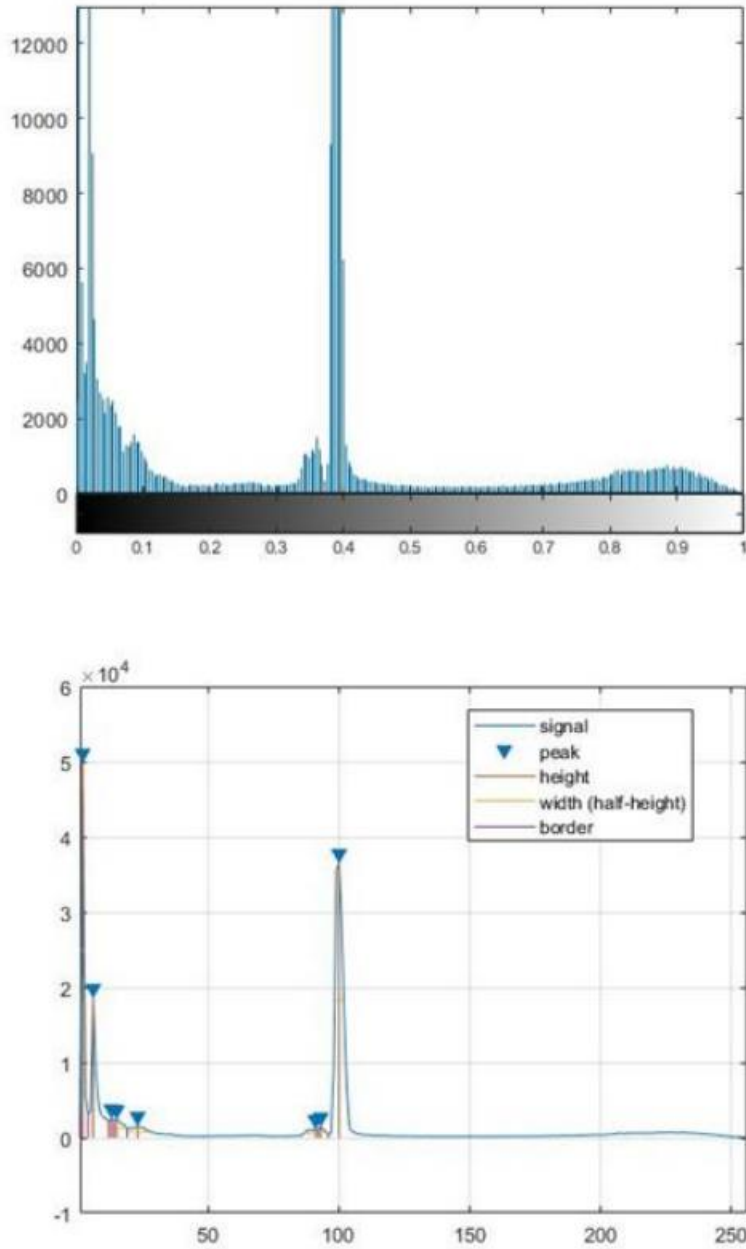


Figure 3: Histogram image of one of the data samples.

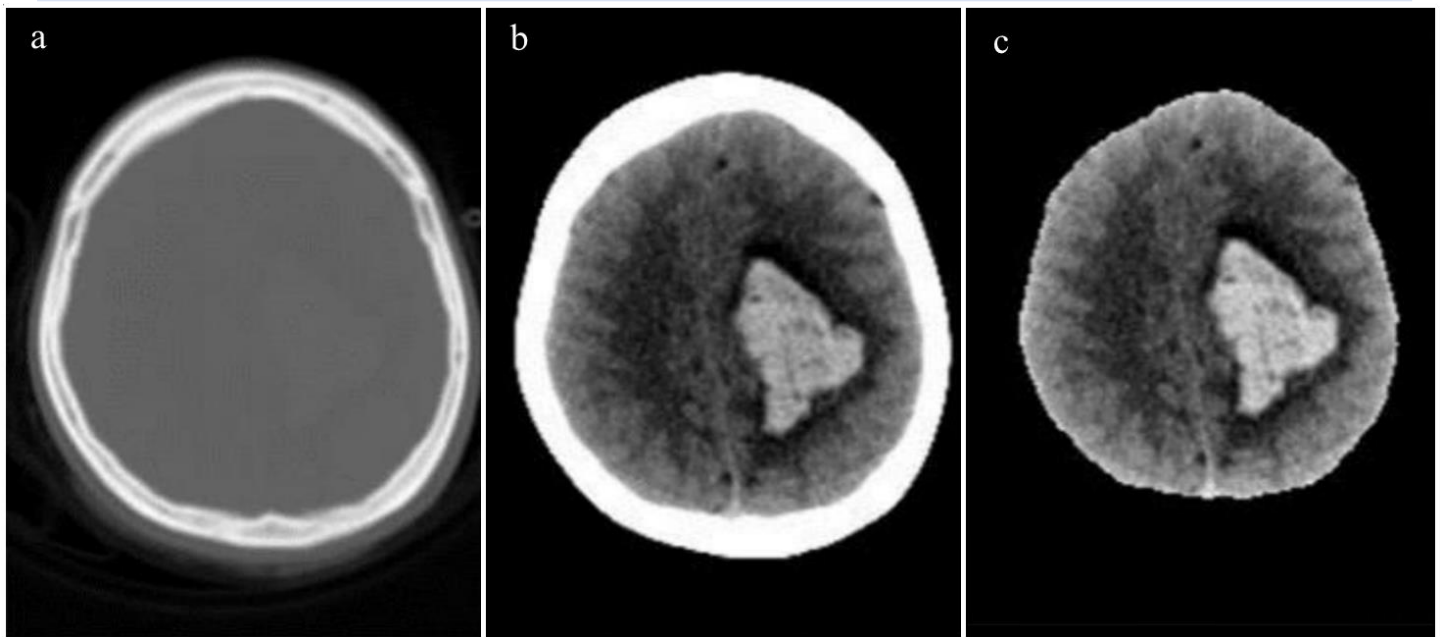


Figure 4: Segmentation using binary thresholding: (a) Original image, (b) enhanced image and (c) final skull removal image.

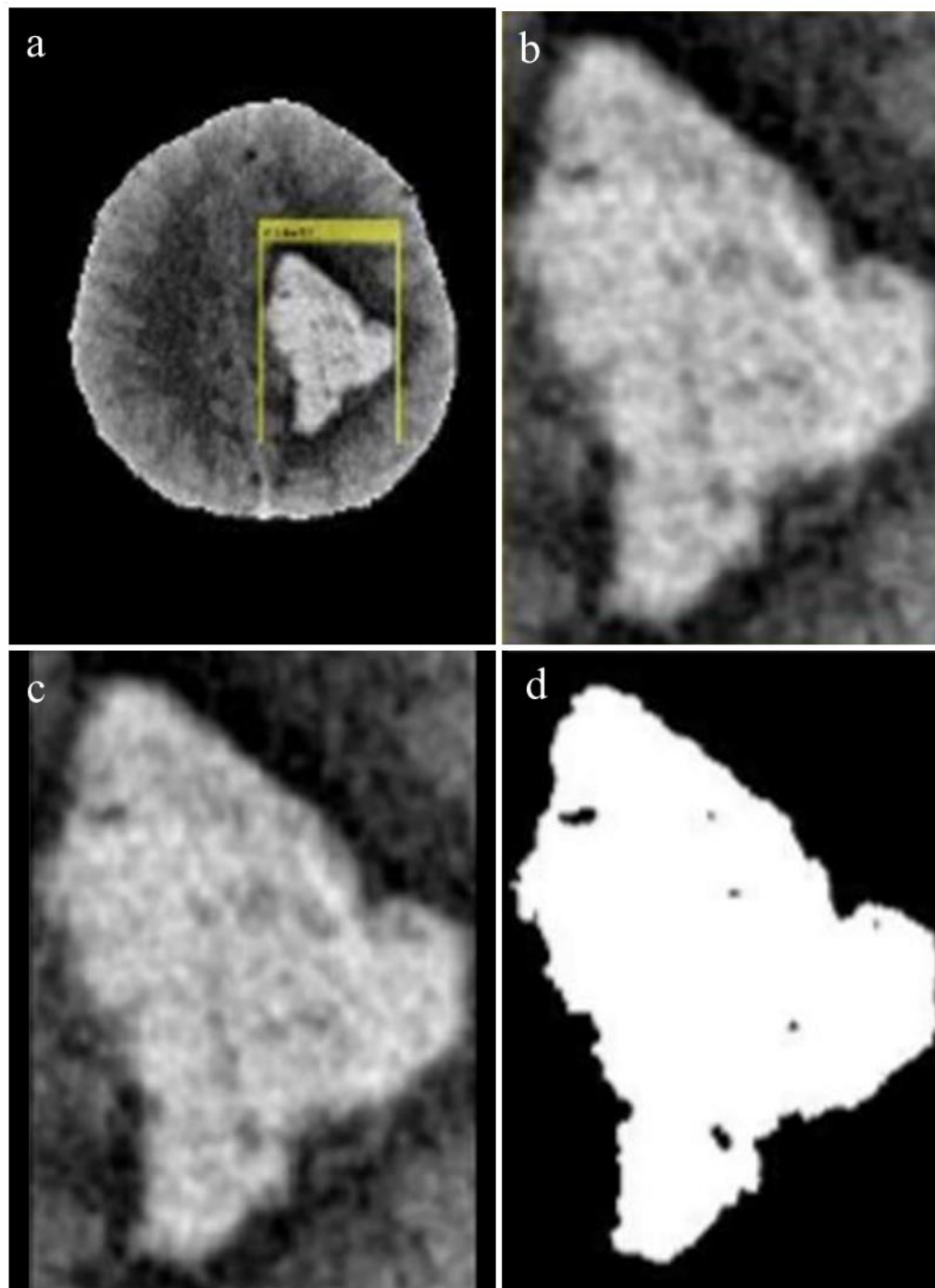


Figure 5: Automated detection and localization of ICH. (a) ICH detection and localization in a coordinate, which then is marked in (b-c) yellow box containing (d) segmented ICH using ICH binary thresholding.

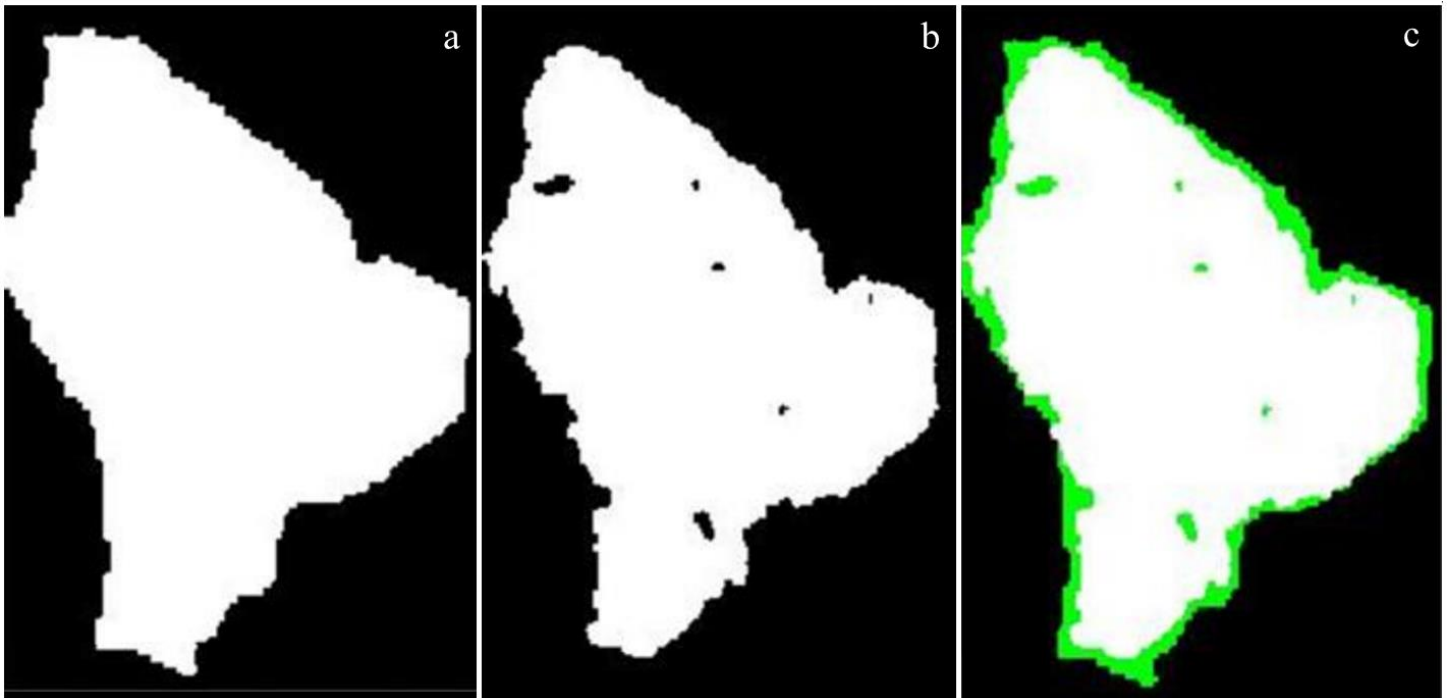


Figure 6: Evaluation of system performance based on manual demarcations and A.I.-based auto-detection. (a) is marked by radiologist, (b) is auto detected and segmented and (c) demonstrates non-overlapping pixels between these two segmented images.

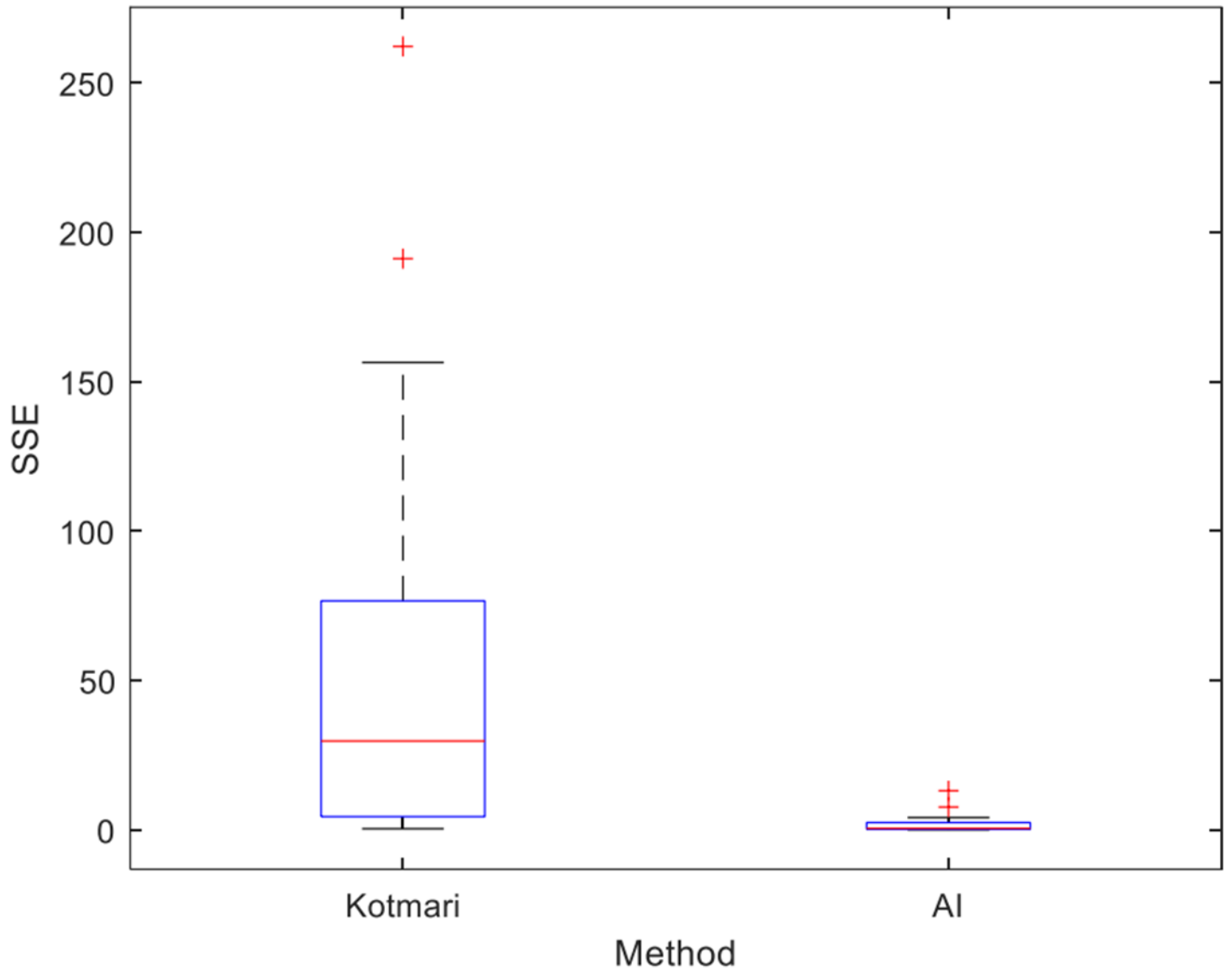


Figure 7: Boxplot showing SSE of Conventional (Kothari) vs G.T. and A.I. vs G.T.

TABLE LEGENDS

Table 1: Dice similarity coefficient of the detected ICH.

Case #	Dice Similarity Coefficient	Case #	Dice Similarity Coefficient	Case #	Dice Similarity Coefficient
011	0.932	043	0.888	095	0.717
012	0.941	044	0.914	102	0.926
013	0.936	052	0.821	103	0.889
014	0.873	061	0.852	111	0.932
015	0.870	071	0.816	112	0.869
023	0.818	072	0.886	113	0.924
024	0.786	073	0.884	114	0.915
032	0.691	074	0.889	115	0.878
033	0.857	075	0.904	121	0.773
034	0.870	092	0.821	122	0.879
035	0.853	093	0.790	123	0.844
042	0.862	094	0.856	124	0.759

Table 2: The ICH sizes using different methods and SSE of all the detected ICH.

Case #	ICH Size (cm ²)			SSE	
	Ground Truth (G.T.)	Kothari	A.I.	Kothari vs G.T.	A.I. vs G.T.
011	13.91	23.26	12.16	87.45	3.07
012	16.75	26.92	14.90	103.57	3.41
013	17.78	31.61	15.74	191.21	4.15
014	16.21	21.94	12.58	32.92	13.13
015	12.23	18.78	9.46	42.88	7.66
023	0.86	2.74	0.60	3.54	0.07
024	0.89	2.04	0.58	1.32	0.09
032	1.99	3.82	1.06	3.36	0.87
033	2.80	4.84	2.11	4.14	0.48
034	3.29	7.32	2.54	16.26	0.56
035	2.90	7.84	2.17	24.38	0.54
042	2.02	7.35	1.54	28.42	0.23
043	2.37	9.95	1.90	57.34	0.22
044	2.17	8.49	1.88	39.82	0.09
052	0.77	0.13	0.54	0.41	0.05
061	3.12	4.85	2.33	2.99	0.63
071	4.47	10.04	3.09	31.10	1.89
072	7.83	13.76	6.26	35.11	2.49
073	8.94	14.85	7.11	34.93	3.35
074	9.95	14.50	7.98	20.67	3.88
075	9.13	12.37	7.55	10.53	2.47
092	1.80	3.71	1.27	3.64	0.28
093	1.74	5.01	1.14	10.68	0.36
094	1.28	3.78	1.03	6.26	0.06
095	0.76	2.94	0.43	4.76	0.11
102	1.29	2.69	1.14	1.94	0.02
103	1.18	2.39	0.95	1.46	0.05
111	5.75	21.94	5.08	262.23	0.44
112	5.59	18.09	4.31	156.45	1.63
113	4.54	16.01	3.92	131.37	0.39
114	3.85	12.94	3.27	82.68	0.34
115	3.11	12.25	2.45	83.51	0.44
121	2.62	7.72	1.66	26.02	0.91
123	3.55	11.13	2.81	57.51	0.54
124	4.27	14.97	3.13	114.65	1.30
125	4.40	12.80	2.71	70.63	2.87